

PREPARED FOR THE U.S. DEPARTMENT OF ENERGY,
UNDER CONTRACT DE-AC02-76CH03073

PPPL-3715
UC-70

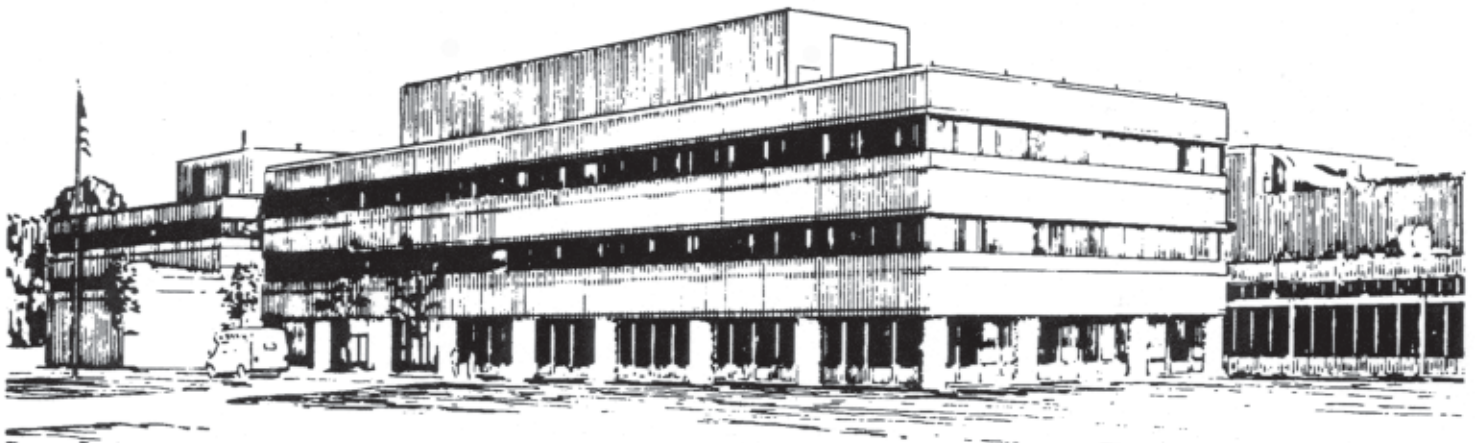
PPPL-3715

**Bounce Precession Fishbones
in the National Spherical Tokamak Experiment**

by

Eric Fredrickson, Liu Chen, and Roscoe White

June 2002



**PRINCETON PLASMA PHYSICS LABORATORY
PRINCETON UNIVERSITY, PRINCETON, NEW JERSEY**

PPPL Reports Disclaimer

This report was prepared as an account of work sponsored by an agency of the United States Government. Neither the United States Government nor any agency thereof, nor any of their employees, makes any warranty, express or implied, or assumes any legal liability or responsibility for the accuracy, completeness, or usefulness of any information, apparatus, product, or process disclosed, or represents that its use would not infringe privately owned rights. Reference herein to any specific commercial product, process, or service by trade name, trademark, manufacturer, or otherwise, does not necessarily constitute or imply its endorsement, recommendation, or favoring by the United States Government or any agency thereof. The views and opinions of authors expressed herein do not necessarily state or reflect those of the United States Government or any agency thereof.

Availability

This report is posted on the U.S. Department of Energy's Princeton Plasma Physics Laboratory Publications and Reports web site in Fiscal Year 2002. The home page for PPPL Reports and Publications is: http://www.pppl.gov/pub_report/

DOE and DOE Contractors can obtain copies of this report from:

U.S. Department of Energy
Office of Scientific and Technical Information
DOE Technical Information Services (DTIS)
P.O. Box 62
Oak Ridge, TN 37831

Telephone: (865) 576-8401
Fax: (865) 576-5728
Email: reports@adonis.osti.gov

This report is available to the general public from:

National Technical Information Service
U.S. Department of Commerce
5285 Port Royal Road
Springfield, VA 22161

Telephone: 1-800-553-6847 or
(703) 605-6000
Fax: (703) 321-8547
Internet: <http://www.ntis.gov/ordering.htm>

Bounce precession fishbones in the National Spherical Tokamak Experiment

Eric Fredrickson¹, Liu Chen², Roscoe White¹

¹*Plasma Physics Laboratory, Princeton University, P.O.Box 451,
Princeton, New Jersey 08543*

²*Department of Physics and Astronomy, University of California, Irvine CA. 92697*

Abstract

Bursting modes are observed on the National Spherical Torus Experiment [M. Ono *et al.*, Nucl. Fusion **40**, 557 (2000)], which are identified as bounce precession frequency fishbone modes. They are predicted to be important in high current, low shear discharges with a significant population of trapped particles with a large mean bounce angle, such as produced by near tangential beam injection into a large aspect ratio device. Such a distribution is often stable to the usual precession-resonance fishbone mode. These modes could be important in ignited plasmas, driven by the trapped alpha particle population.

PACS numbers: 52.35.Py 52.40.Mj

/Publication/Eric/bfish.tex

I. Introduction

Resonant interaction of high energy particles with magnetic perturbations in toroidal devices can produce large scale modification of the particle distribution, sometimes leading to particle loss. A well known example of this is the fishbone mode¹⁻⁴, first observed as a resonance with the mean trapped particle toroidal precession, and later found to be possible also as a resonance with passing particles at the transit frequency⁵⁻⁷. In this work we wish to report the observation of a strong resonant fishbone interaction at the trapped particle bounce frequency.

In Fig. 1 is shown a sequence of chirping modes observed on the National Spherical Torus Experiment (NSTX)⁸ in shot number 108794. The colors of the contours indicate the toroidal mode numbers, with black, red, green, blue and yellow representing $n = 1$ to 5, respectively. The modes we wish to discuss are those at $t = 0.145, 0.19, 0.24$ and 0.26 sec which are identified to have toroidal mode numbers of $n = 1, 2, 3, 4$ respectively. The strong frequency chirping indicates that the mode frequency is determined by the particle distribution rather than by equilibrium parameters alone, such as in the case of a Toroidal Alfvén Eigenmode (TAE)⁹, and are thus Energetic Particle Modes (EPM)¹⁰, which we identify as fishbone modes. The black band between 0.11 and 0.18 s, and between 50 and 80 kHz are also bursting, chirping modes. The fishbone activity is very commonly observed with neutral beam injection in the early phase of NSTX discharges during the plasma current ramp (Fig. 2). Only the three strongest bursts are correlated with modest drops in the neutron rate.

The oscillations, particularly from the larger amplitude bursts, may be observed in the soft x-ray emission. A cross section of the NSTX with the locations of the soft x-ray camera chords and the poloidal array of the Mirnov coils is shown in Fig 3. In Fig. 4 a are shown the soft x-ray data from the lower camera during the period 0.14 to 0.15 s encompassing the first large, lower frequency fishbone burst. The fluctuations are visible mainly on chords viewing the plasma at about the half radius. For reference in Fig. 4b is shown the external poloidal magnetic field fluctuation amplitude and in Fig. 4c are shown the chord integrated

soft x-ray emission profile and the inferred q profile from EFIT¹¹. The (inverted) soft x-ray emissivity profile is hollow, with a peak at a minor radius of about $0.2m$ and the emissivity is very low outside a minor radius of about $0.4m$. Thus the soft x-ray camera data is most useful in the limited radial range between $0.2m$ and $0.4m$. Over this limited range the soft x-ray data indicates that the mode has a kink-like structure; the phase inversion at $r = 0.2m$ is likely due to the hollow emissivity profile.

There is no direct measurement of the field helicity q ; it is inferred via fitting of the magnetics data with the code EFIT¹¹. The central q is estimated to be near or slightly less than two at the first large fishbone burst (Fig. 2b-d at $0.142s$). This numerical fit indicates that the q profile is fairly flat in the core, and becomes progressively more so during the period of these modes.

In Fig. 4c q is close to two over the region $0.2m < r < 0.4m$, suggesting that the mode has some significant $m = 2, n = 1$ component. However, strong coupling to higher m values, as is generally the case for kink-like modes, is suggested by the relatively short poloidal wavelength measured by the poloidal array of Mirnov coils. In Fig. 5 is shown the relative phase shift vs. poloidal angle of the Mirnov coils for this mode. The array is incomplete, but where present the phase shifts can be fit with an effective poloidal mode number of about 6 whereas the actual poloidal mode number could be much higher, indicating coupling to higher m values.

The neutron production in NSTX is predominantly from beam-target reactions, thus the neutron rate is a measure of the fast ion population. There is no detectable correlation of neutron rate changes co-incident with most of the fishbone bursts, indicating that the fishbones do not substantially impact the most energetic fast ion population, which produce the bulk of the neutrons. However, as will be seen, the fishbones are predicted to mainly interact with fast ions nearer to 20 keV (rather than the full energy fast ions of 80 keV). Relatively few neutrons are produced by those lower energy beam ions.

II. Mode Particle Interaction

The analysis of the resonant interaction of high energy particles with magnetohydrodynamic (MHD) modes is well known¹². Perturb the equilibrium field \vec{B} with a perturbation of the form $\vec{b} = \nabla \times \alpha \vec{B}$ and also introduce an electric perturbation Φ . Consider a particular harmonic of the wave, of the form

$$\alpha = \alpha_{mn} e^{i(n\zeta - m\theta - \omega t)} \quad \Phi = \Phi_{mn} e^{i(n\zeta - m\theta - \omega t)}. \quad (1)$$

where θ and ζ are poloidal and toroidal angles, respectively and ω is the mode frequency. We consider a MHD mode, in which case α_{mn} and Φ_{mn} are related. Using $\nabla \times \vec{E} = -\partial_t \vec{B}$ we find for the electric field $\vec{E} = -\partial_t \alpha \vec{B} - \nabla \Phi = -i\omega \alpha_{mn} e^{i(n\zeta - m\theta - \omega t)} \vec{B} - \nabla \Phi$. The rapid mobility of electrons shorts out E_{\parallel} in a time short compared to the Alfvén time, so $E_{\parallel} = -i\omega B \alpha_{mn} e^{i(n\zeta - m\theta - \omega t)} - \vec{B} \cdot \nabla \Phi / B = 0$. Using the Boozer¹³ representation for the equilibrium field, $\vec{B} = \mathbf{g}(\psi) \nabla \zeta + \mathbf{I}(\psi) \nabla \theta + \delta \nabla \psi$ with ψ the toroidal flux, we find $\omega \alpha_{mn} = (nq - m) \Phi_{mn} / (gq + I)$. The resonant change in the kinetic energy of a particle due to the wave is due to the drift motion, and can be written as

$$\frac{dE}{dt} = i \left[-n\dot{\zeta}_d + m\dot{\theta}_d \right] \Phi_{mn} e^{i(n\zeta - m\theta - \omega t)} - \Phi'_{mn} \dot{r} e^{i(n\zeta - m\theta - \omega t)} \quad (2)$$

with $\dot{\zeta}_d$, $\dot{\theta}_d$, \dot{r} the drift motion, r the minor radius, and prime indicates differentiation with respect to r .

Although the bounce frequency ω_b changes significantly with increasing bounce angle θ_b , the bounce motion continues to be dominated by the fundamental harmonic $\theta = \theta_b \sin \omega_b t$. For a pendulum the leading correction to the harmonic content is $\theta = (\theta_b + \Delta) \sin \omega_b t + \Delta \sin 3\omega_b t$ with $\Delta = \theta_b^3 / 192$ while the correction to the bounce frequency is $\omega_b = 1 - \theta_b^2 / 16$, normalized to the small angle bounce frequency. Similarly, direct simulation shows that in NSTX even for bounce angle of $\theta_b = 2.5$ the higher harmonics are an order of magnitude smaller than the fundamental.

Thus for trapped particles write $\theta = \theta_b \sin \omega_b t$, $\zeta = q\theta_b \sin(\omega_b t) + \omega_p t$, $r = r_0 + \rho_b e^{i\omega_b t}$ with r_0 the banana center, ρ_b the banana width, and note $\langle \dot{\zeta}_d \rangle = \omega_p$, the precession fre-

quency, with $\langle F \rangle$ indicating bounce averaging of F and use the usual Bessel expansion $e^{ia\theta} = \sum_l J_l(a\theta_b)e^{il\omega_b t}$ to find for the bounce averaged energy change of a trapped particle

$$\frac{d\mathcal{E}}{dt} \simeq -in\omega_p\Phi_{mn} \sum_l J_l((nq-m)\theta_b)e^{iQ_l} - i\omega_b\rho_b\Phi'_{mn} \sum_l J_l((nq-m)\theta_b)e^{iQ_{l+1}} \quad (3)$$

where $Q_l = n\omega_p t + l\omega_b t - \omega t$. Resonance requires secularity, or $Q \simeq \text{constant}$. This condition is strongly dependent on the equilibrium and the particle energy. The bounce frequency is proportional to the particle velocity and inversely proportional to q . The precession frequency is proportional to the particle energy and q , and inversely proportional to the field strength, and also decreases and can even change sign due to the formation of a magnetic well at high beta. Both frequencies are also strong functions of the bounce angle θ_b .

The dominant resonant frequency in this energy exchange is thus determined by the particle distribution, the field strength, the radial dependencies of Φ_{mn} , q and the bounce and precession frequencies. In previous observed cases the fishbone, which was primarily an $n=1, m=1$ mode, has been dominated by the $\omega_p\Phi_{mn}$ term with $l=0$, giving a resonance at $\omega \simeq n\omega_p$, the precession frequency. However this term is also resonant at $\omega = n\omega_p \pm \omega_b$ for $l = \pm 1$, and the $\rho_b\Phi'_{mn}$ term is also resonant at $\omega = n\omega_p + \omega_b$ for $l=0$. For trapped particles with large bounce angle the value of J_1 can be comparable to J_0 . Depending on thresholds, growth rates, and the relative magnitudes of ω_p , ω_b , and Φ_{mn} , $\rho_b\Phi'_{mn}$ the bounce averaged energy transfer due to different terms can dominate the mode-particle energy exchange, producing a mode with a frequency other than the precession frequency.

Assuming the resonance at $\omega = n\omega_p + \omega_b$ dominates we have

$$\frac{dE}{dt} = A \sin(Q) \quad \frac{dQ}{dt} = n\omega_p + \omega_b - \omega \quad (4)$$

with $A \simeq \omega_p\Phi_{mn}J_1((m-nq)\theta_b) + \rho_b\omega_b\Phi'_{mn}J_0((m-nq)\theta_b)$. Note that the ratio of the two terms in A is independent of particle energy, depending only on equilibrium parameters, bounce angle, particle position r , and mode structure. Expand $dQ = \partial_E Q(E - E_0)dt$ about the resonance $n\omega_p + \omega_b = \omega$, and use $\partial_E \omega_p = \omega_p/E$, $\partial_E \omega_b = \omega_b/2E$, giving an island in energy of the form $(E - E_0)^2/2 = c - 2k \cos Q$ with $k = EA/(2n\omega_p + \omega_b)$ and all quantities evaluated at

the resonance $n\omega_p + \omega_b = \omega$. This resonance island, existing in the energy variable, the radial variable, and the frequency, causes nonreversible energy transfer between the wave and the particle distribution, provided either energy or radial gradients exist in the distribution¹⁴.

III. Comparison with Experiment

We have used numerical equilibria and beam particle distributions generated by TRANSP¹⁵ and the guiding center code ORBIT^{16,17} to compare with the experimental results shown above. TRANSP was used both to create the parameters for numerical equilibria representing the plasma at the times of the fishbone bursts, and also to provide a Monte-Carlo list of energy, pitch, and location of ten thousand beam particles for each burst. The code ORBIT was then used for an analysis of the particle distribution in these equilibria, determining whether particles were passing or trapped, and finding bounce angles, bounce frequencies, and precession rates for each trapped particle. The list of ten thousand beam particles gives reasonably good statistics for the determination of the instantaneous properties of the beam at the time of the fishbone. Particles above $50keV$ are practically all passing. In Fig. 6 is shown the bounce frequency $f_b = \omega_b/2\pi$ and precession frequency $f_p = \omega_p/2\pi$ of the trapped particle component of the beam at the time of the $n = 1$ burst, $t = 0.145sec$. The upper envelope of the bounce frequency points is proportional to the square root of the energy as expected. Seven percent of the beam is trapped, with a mean precession frequency of about $9kHz$ and a mean bounce angle of $\theta_b = 0.84$. The lines are least square fits to the data sets. The range of plasma frame mode frequencies during chirping matches the distribution of precession frequencies. At this time $q(0) = 2$ and $q = 3$ occurs at $r/a = 0.65$. The low mode frequency leads to an interpretation of this mode as a precession frequency fishbone with $n = 1, l = 0$. The small value of the mean bounce angle for the distribution and relatively large precession frequency make probable a dominant contribution of the $\omega_p \Phi_{11} J_0$ term to the energy exchange.

The bursts occurring later in the discharge, with $n = 2,3,4$, cannot be so interpreted. As

the discharge evolves, the q profile becomes lower and flatter, the plasma beta increases, the trapped particle fraction increases, and the mean bounce angle increases. The beam distribution also has a larger population of high energy particles at later times in the discharge, so the average beam energy increases. In Table 1 are shown the equilibrium, fishbone and beam properties at the times of the bursts shown in Fig. 1. The toroidal mode numbers and the frequency ranges of the fishbone bursts are taken from Fig. 1. The q profile is given by TRANSP. The trapped fraction, mean bounce and precession frequencies, bounce angle, and mean trapped particle energy $\langle E \rangle$ were calculated using the TRANSP supplied beam particles and the code ORBIT.

In Fig. 7 are shown the bounce and precession frequencies of the trapped particle component of the beam for the $n = 4$ burst at $t = 0.26\text{sec}$. At this time there are a large number of negatively precessing particles, and the mean precession frequency is much smaller than the bounce frequency. Intermediate times, $t = 0.24\text{sec}$ and $t = 0.26\text{sec}$ are almost linear interpolations between Figs. 6 and 7.

By comparing the experimental mode frequencies with the range of bounce and precession frequencies at the time of each fishbone, we identify the $n = 1$ mode to be a conventional precession frequency fishbone mode, and the higher n modes to be bounce precession modes with $l = 1$. The plasma rotation frequency is about 4.5kHz at the $q = 2$ surface, so this value should be subtracted from the experimental frequencies. In Fig. 8 is shown for each mode n the strength of the resonance at frequency f , with $f = nf_p + lf_b$. The bounce frequency f_b enters into each mode with $l = 1$, except for $n = 1$, where $l = 0$. The width of the vertical column at a given height above each value of n is proportional to the energy transfer at that frequency, given by the number density of beam particles resonant at that frequency times the frequency. We used frequency intervals of 3kHz and determined the number of particles in the Monte Carlo distribution with a resonant frequency in each interval. The width of the column thus is proportional to the existing drive for an EPM mode at that frequency. Because a fishbone is most unstable at high frequency, we expect the fishbone mode at each n to chirp downward through that part of the column with substantial width. As that part

of the distribution which is resonant at a particular frequency is flattened the mode moves on to the free energy available at a slightly lower frequency, continuing this process until the available free energy is depleted, either by induced particle loss or simply by local flattening of the distribution. The frequency ranges obtained in this way are in good agreement with the observed range of chirping seen in Fig. 1.

In Fig. 9 is shown the beam content vs energy for $t = 0.26\text{sec}$, using bins of 10keV each, normalized to the total number in the low energy bin $0 < E < 10\text{keV}$. We observe that the mode can be driven only by the low energy beam particles and thus the expected loss of particles should be from the population below 20keV , which would not cause a drop in neutron flux. This is also confirmed by the fact that the frequency chirping does not extend to the bounce frequencies of particles above $\sim 40\text{keV}$.

IV. Approximate Dispersion relation

Analytical insight concerning the detailed mode excitation can be obtained by assuming $m \simeq nq > 1$, weak shear, and keeping the finite banana width effect with respect to the radial scale length. We thus may adopt the ballooning representation as an analytical approximation. In this case the mode is well localized radially, and the $\omega_b \rho_b \Phi'_{mn} J_0$ term should dominate the energy exchange. The corresponding dispersion relation has been previously derived¹⁸ and is given by

$$-i \frac{\omega}{\omega_A} + \delta W_f + \delta W_k = 0 \quad (5)$$

where $\omega_A = v_A/qR$, δW_f is the usual incompressible ideal MHD fluid δW . Retaining only the dominant bounce resonance due to the trapped energetic particles we have

$$\delta W_k = \frac{\pi^2 e^2 q R_0 B_0}{m c^2 s} \int \frac{dE d\mu \theta_b^2 \Omega_p^2 \tau_b K F_0}{\Delta_b (1 + \Delta_b^2)^{3/2}} \frac{\omega - n\omega_p}{\omega_b^2 - (\omega - n\omega_p)^2} \quad (6)$$

where $E = v^2/2$, $\mu = v_\perp^2/2B_0$, $\Omega_p^2 = (v_\perp^2/2 + v_\parallel^2)/\omega_c R_0$, τ_b is the bounce period, $\tau_b = 2\pi/\omega_b$, and $\Delta_b = (\theta_b k_\theta \rho_b)/2^{3/2}$ denotes the finite banana width (ρ_b) effect. Here $s = rq'/q$ is the magnetic shear and $K F_0 = (\omega \partial_E + \hat{\omega}_*) F_0$ with $\hat{\omega}_* F_0 = \vec{k} \times \hat{e}_\parallel / \omega_c \cdot \nabla F_0$. Other notation

is standard. In the present case, δW_k is due to the energetic beam ions. Note that Eq. 5 takes the form of the generic fishbone dispersion relation³ and thus one can anticipate similar stability properties, such as instability threshold when the drive due to the pressure inhomogeneity $\hat{\omega}_* F_0$ at the $\omega \simeq \omega_b + n\omega_p$ wave bounce precession resonance exceeds the dissipation due to the Alfvén resonance absorption $-i\omega/\omega_A$. To be more specific, we take F_0 to be a slowing down distribution with a single pitch angle and proximity to MHD marginal stability, we then find the unstable mode has $\omega_r \simeq 0.83(\omega_{bm} + n\omega_p)$, and the threshold condition is given by $\alpha_E = q^2 R_0 \beta'_E > \alpha_{Ec} = 0.48s(\omega_{bm} + n\omega_{pm})/\theta_b \omega_A$, with ω_{bm}, ω_{pm} the bounce and precession frequencies evaluated at the maximum energy of F_0 and β_E the beam beta. In the present case the above dispersion relation should correspond to local values where the beam drive α_E is a maximum, ie around $q = 2$. Thresholds and frequencies are consistent with experimental observations. The fact that the threshold is proportional to the shear, not the case for the usual precession frequency fishbone, probably contributes to the dominance of the bounce frequency mode in these discharges, which have values of shear less than one. Note that this condition makes the mode particularly important for high q and low shear, commonly referred to as advanced tokamak operation.

V. Conclusion

Without more detailed knowledge of the form of the perturbation, obtained either from experimental data or from a more detailed stability analysis, it is impossible to assess the dominant mechanism for mode-particle interaction in a given case, ie to know which of the Bessel function terms are most important, and to have clear predictions concerning stability thresholds. In other discharges with higher values of q and lower field strength, the bounce and precession rates are much more equal in magnitude. There appears to be a great variety of possible frequencies for these modes.

We have carried out simulations of the effect of the modes on the beam distribution at $t = 0.26\text{sec}$, using mode content of $m/n = 1/1$, and $2/1$ rotating at 50kHz . Modes

of amplitude $\delta B/B = 10^{-3}$ do not produce any particle loss, only a modification of the distribution. This could be due to the variation of ω_b radially, causing particles to quickly move out of resonance as they are moved outwards, or due to the fact that the particles interacting with the mode are of rather low energy.

In an ignited plasma, with the alpha particles isotropic at birth, the mode should instead be driven by and act upon the high energy alphas, which could produce a significant redistribution of the alpha population.

This work was supported by the U.S. Department of Energy Grant DE-FG03-94ER54271 and under contract number DE-AC02-76-CHO3073 and NSF Grant ATM-9971529.

REFERENCES

1. PDX Group, Princeton Plasma Physics Lab, *Phys Rev. Lett* **50**, 891 (1983).
2. R. B. White, R. J. Goldston, K. McGuire, A. H. Boozer, D. A. Monticello, and W. Park *Phys Fluids* **26**, 2958 (1983).
3. L. Chen, R. B. White, and M. N. Rosenbluth *Phys Rev. Lett* **52**, 1122 (1984).
4. B. Coppi and F. Porcelli *Phys Rev. Lett* **57**, 2272 (1986).
5. W. W. Heidbrink, K. Bol, D. Buchanauer et al *Phys Rev. Lett* **57**, 835 (1986).
6. R. Betti and J. P. Freidberg *Phys Rev. Lett* **70**, 3428 (1993).
7. Ya. I. Kolesnichenko, V. S. Marchenko, R. B. White *Phys Plasmas* **8**, 3143 (2001).
8. M. Ono *et al Nucl Fusion* **40**, 557 (2000).
9. C. Z. Cheng, L. Chen, and M. S. Chance, *Ann. Phys.* **161**, 21 (1985).
10. L. Chen, *Phys. Plasmas* **1**, 1519 (1994), F. Zonca and Liu Chen, *Phys. Plasmas* **3**, 323 (1996), N. N. Gorelenkov, C. Z. Chang, and W. M. Tang, *Phys. Plasmas* **5**, 3389 (1998)
11. L.L. Lao, H. St. John, R. D. Stambaugh, A. G. Kellman, and W. Pfeiffer *Nucl Fusion* **25**, 1611 (1985).
12. R.B. White, "The theory of toroidally confined plasmas", (Imperial College Press, London, 2001) p 237.
13. A. H. Boozer, *Phys. Fluids* **24**, 1999 (1981).
14. T. O'Neil, *Phys. Fluids* **12**, 2255 (1965).
15. R. V. Budny, M. G. Bell A. C. Janos *et al, Nucl Fusion* **35**, 1497 (1995).
16. R.B. White and M. S. Chance, *Phys. Fluids* **27** 2455 (1984).
17. R.B. White, *Phys. Fluids B* **2**(4), 845 (1990).
18. S. T. Tsai and L. Chen *Phys. Fluids B* **5**(9), 3284 (1993).

Table I. Fishbone and Beam Properties

time sec	0.145	0.19	0.24	0.26
toroidal n	1	2	3	4
range kHz	2 – 10	30 – 70	40 – 110	50 – 120
$q(0)$	2	1.5	1.3	1.2
$r/a(q=2)$	0	.6	.8	.9
% trapped	7	12	15	14
f_b kHz	36	43	56	58
f_p kHz	9	6.7	5.7	5.6
θ_b	0.84	1.1	1.2	1.2
$\langle E \rangle$ keV	14.2	16.4	21	22

Figure Captions

Fig. 1 NSTX fishbones seen at $t = 0.145, 0.19, 0.24, 0.26 \text{ sec}$, with $n = 1, 2, 3, 4$ respectively.

Fig. 2 Trapped particle bounce (red) and precession (blue) frequencies at $t = 0.145 \text{ sec}$.

Fig. 3 Trapped particle bounce (red) and precession (blue) frequencies at $t = 0.26 \text{ sec}$.

Fig. 4 Energy transfer between mode and beam particles at frequency f , with $f = nf_p + lf_b$

Fig. 5 Beam number vs energy, showing total and trapped fraction, at $t = 0.26 \text{ sec}$.

Table Caption

Equilibrium, burst information, and beam statistics for the fishbone modes seen in Fig. 1

FIGURES

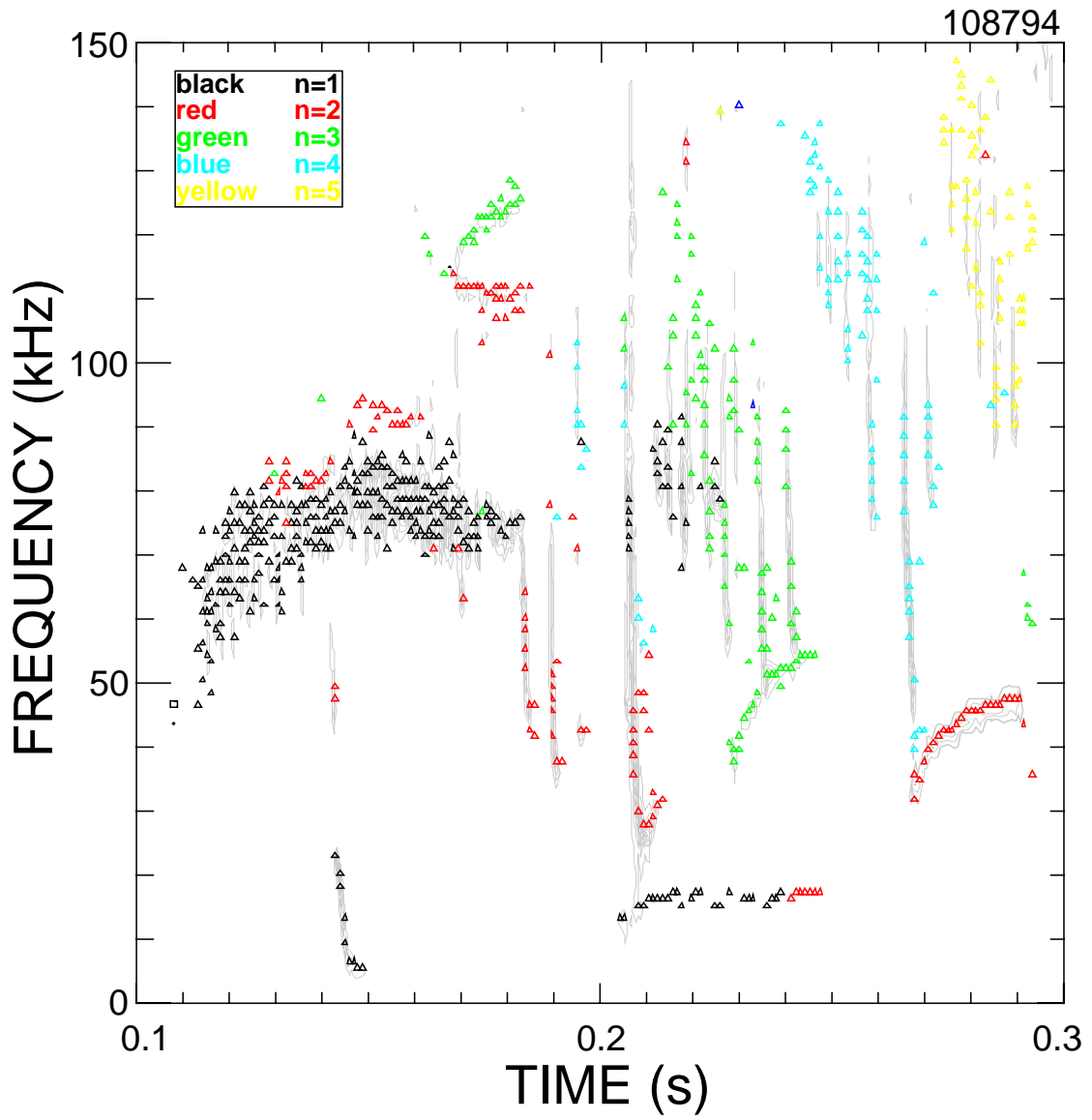


Fig. 1.

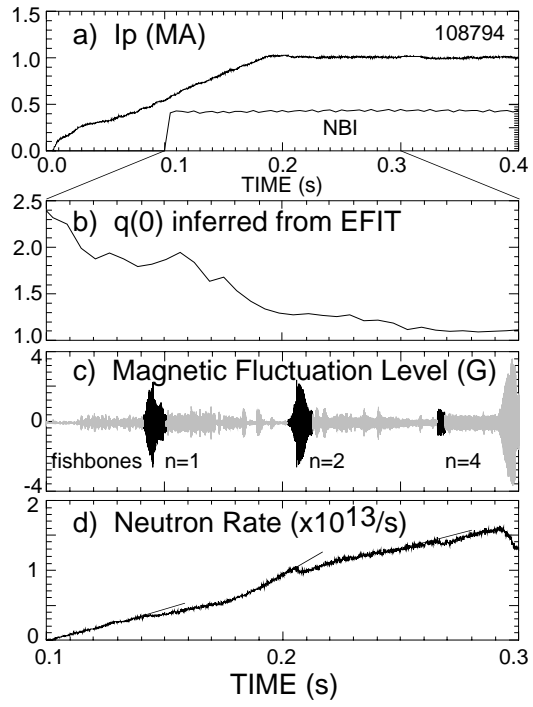


Fig. 2.

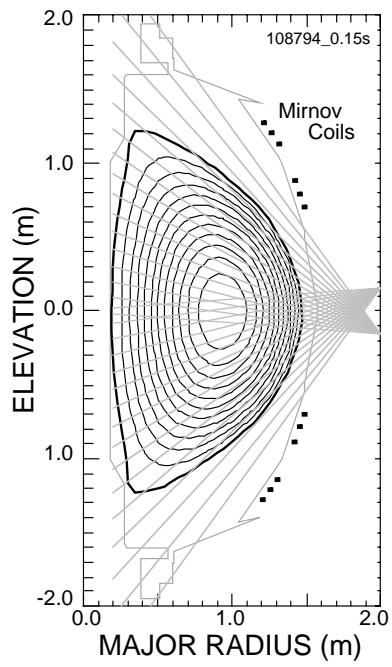


Fig. 3.

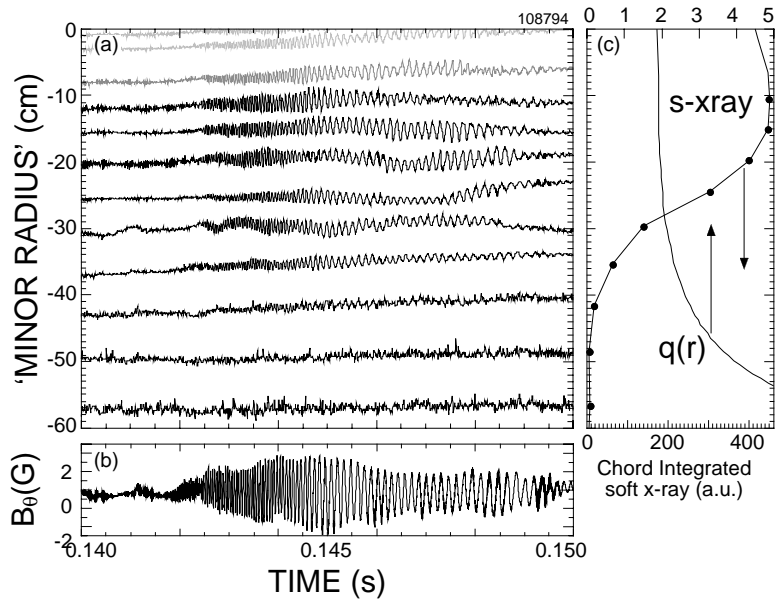


Fig. 4.

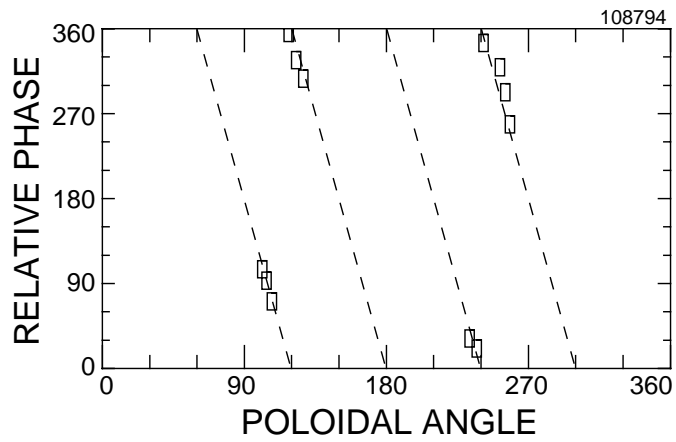


Fig. 5.

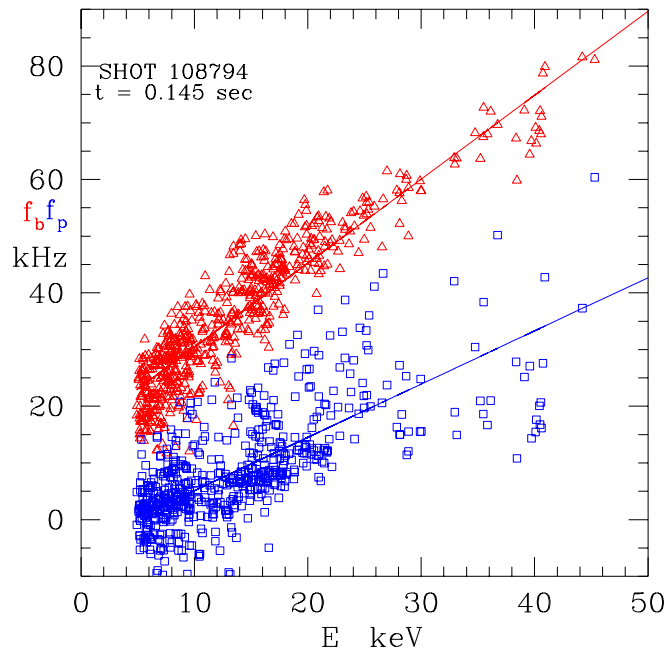


Fig. 6.

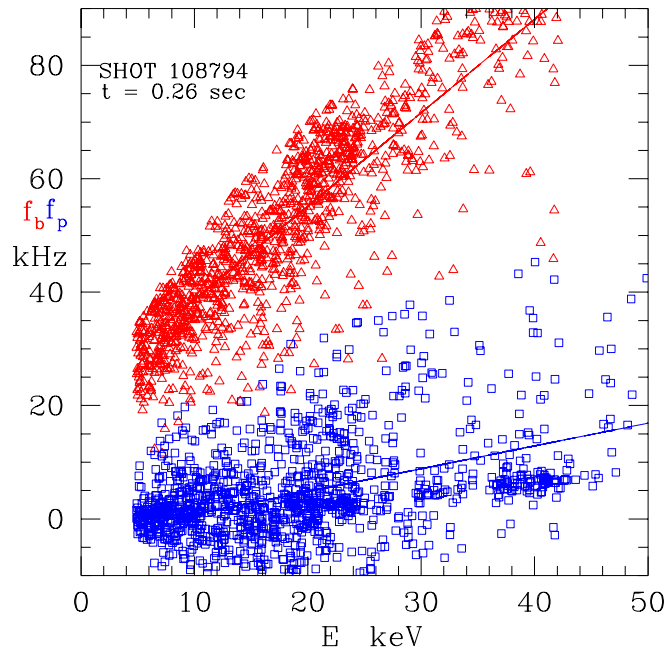


Fig. 7.

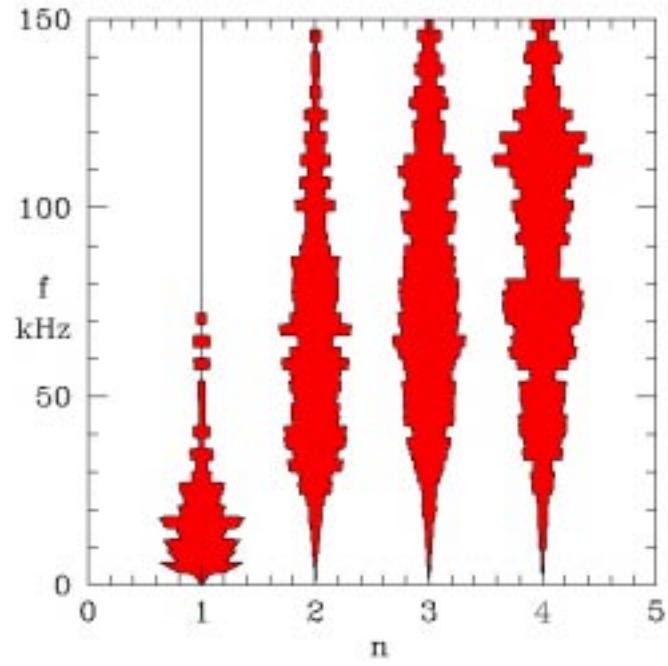


Fig. 8.

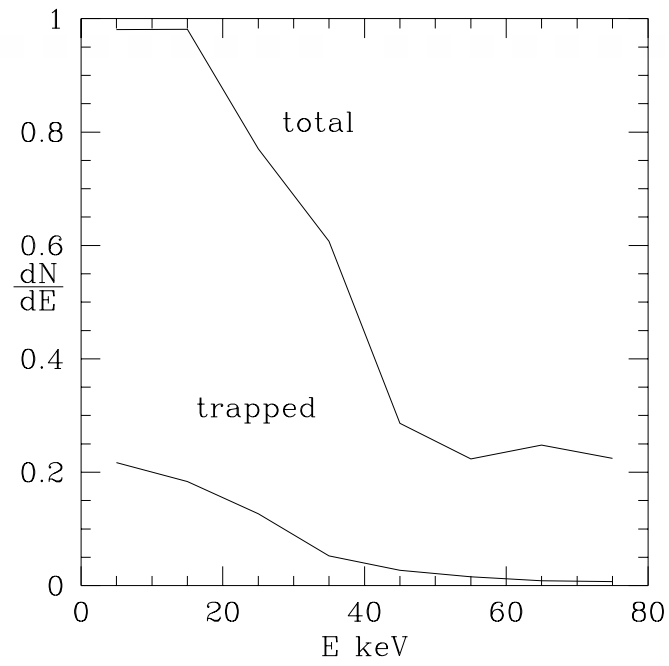


Fig. 9.

External Distribution

Plasma Research Laboratory, Australian National University, Australia
Professor I.R. Jones, Flinders University, Australia
Professor João Canalle, Instituto de Fisica DEQ/IF - UERJ, Brazil
Mr. Gerson O. Ludwig, Instituto Nacional de Pesquisas, Brazil
Dr. P.H. Sakanaka, Instituto Fisica, Brazil
The Librarian, Culham Laboratory, England
Library, R61, Rutherford Appleton Laboratory, England
Mrs. S.A. Hutchinson, JET Library, England
Professor M.N. Bussac, Ecole Polytechnique, France
Librarian, Max-Planck-Institut für Plasmaphysik, Germany
Jolan Moldvai, Reports Library, MTA KFKI-ATKI, Hungary
Dr. P. Kaw, Institute for Plasma Research, India
Ms. P.J. Pathak, Librarian, Institute for Plasma Research, India
Ms. Clelia De Palo, Associazione EURATOM-ENEA, Italy
Dr. G. Grosso, Instituto di Fisica del Plasma, Italy
Librarian, Naka Fusion Research Establishment, JAERI, Japan
Library, Plasma Physics Laboratory, Kyoto University, Japan
Research Information Center, National Institute for Fusion Science, Japan
Dr. O. Mitarai, Kyushu Tokai University, Japan
Library, Academia Sinica, Institute of Plasma Physics, People's Republic of China
Shih-Tung Tsai, Institute of Physics, Chinese Academy of Sciences, People's Republic of China
Dr. S. Mirnov, TRINITI, Troitsk, Russian Federation, Russia
Dr. V.S. Strelkov, Kurchatov Institute, Russian Federation, Russia
Professor Peter Lukac, Katedra Fyziky Plazmy MFF UK, Mlynska dolina F-2, Komenskeho
Univerzita, SK-842 15 Bratislava, Slovakia
Dr. G.S. Lee, Korea Basic Science Institute, South Korea
Mr. Dennis Bruggink, Fusion Library, University of Wisconsin, USA
Institute for Plasma Research, University of Maryland, USA
Librarian, Fusion Energy Division, Oak Ridge National Laboratory, USA
Librarian, Institute of Fusion Studies, University of Texas, USA
Librarian, Magnetic Fusion Program, Lawrence Livermore National Laboratory, USA
Library, General Atomics, USA
Plasma Physics Group, Fusion Energy Research Program, University of California at San
Diego, USA
Plasma Physics Library, Columbia University, USA
Alkesh Punjabi, Center for Fusion Research and Training, Hampton University, USA
Dr. W.M. Stacey, Fusion Research Center, Georgia Institute of Technology, USA
Dr. John Willis, U.S. Department of Energy, Office of Fusion Energy Sciences, USA
Mr. Paul H. Wright, Indianapolis, Indiana, USA

The Princeton Plasma Physics Laboratory is operated
by Princeton University under contract
with the U.S. Department of Energy.

Information Services
Princeton Plasma Physics Laboratory
P.O. Box 451
Princeton, NJ 08543

Phone: 609-243-2750
Fax: 609-243-2751
e-mail: pppl_info@pppl.gov
Internet Address: <http://www.pppl.gov>